Dalton Transactions

Accepted Manuscript

This is an *Accepted Manuscript*, which has been through the RSC Publishing peer review process and has been accepted for publication.

Accepted Manuscripts are published online shortly after acceptance, which is prior to technical editing, formatting and proof reading. This free service from RSC Publishing allows authors to make their results available to the community, in citable form, before publication of the edited article. This *Accepted Manuscript* will be replaced by the edited and formatted *Advance Article* as soon as this is available.

To cite this manuscript please use its permanent Digital Object Identifier (DOI®), which is identical for all formats of publication.

More information about *Accepted Manuscripts* can be found in the **Information for Authors**.

Please note that technical editing may introduce minor changes to the text and/or graphics contained in the manuscript submitted by the author(s) which may alter content, and that the standard **Terms & Conditions** and the **ethical guidelines** that apply to the journal are still applicable. In no event shall the RSC be held responsible for any errors or omissions in these *Accepted Manuscript* manuscripts or any consequences arising from the use of any information contained in them.

Journal Name

Dalton Transactions

Dynamic Article Links ►

Cite this: DOI: 10.1039/c0xx00000x

www.rsc.org/xxxxxx

ARTICLE TYPE

An Insight into the Role of the Surfactant CTAB in the Formation of Microporous Molecular Sieves

Dongdong Xu†, Ji Feng†and Shunai Che*

Received (in XXX, XXX) Xth XXXXXXXXX 20XX, Accepted Xth XXXXXXXXX 20XX

DOI: 10.1039/b000000x

Quaternary ammonium salts are well-known zeolite structure-directing agents. However, cationic surfactants with quaternary ammonium head groups are known to fail to function as SDAs of zeolites because their long surfactant chains disrupt the ordered growth of the zeolite crystals. In this study, we found that ZSM-5 and silicalite-1 can be formed very easily with proper synthesis compositions over a large temperature range of 100-200 ˚C. The ^{13}C CP/MAS data for surfactants in ZSM-5 combined with elemental analysis indicated that the surfactants were in more rigid, isolated environments and did not undergo decomposition. The surfactant head groups can serve as structure-directing agents for zeolites, and the long chains become isolated and occupy the micropores. Our findings provide a new insight into the molecular factors governing the formation of inorganic-organic microporous materials, which opens up new possibilities for the elaborate fabrication of mesoporous zeolites.

Introduction

It is well known that many zeolites can be made using organic compounds.[1-4] In particular, quaternary ammonium salts are well known zeolite structure-directing agents (SDAs), which act as (i) space-filling species, (ii) structural directing agents, or (iii) templates.[5-6] The zeolite framework appears to form around these salts, in some cases encapsulate them with a very close fit between the organic groups and the pore walls.[7] The steric requirements limit the number of organic units that can be accommodated and the geometric match between the framework and the template.[8-13] The templates, such as quaternary salts, also act as charge-balancing cations, which impose a restriction on the zeolite framework charge density to compensate the anionic Al-sites.[14-18]

When the alkyltrimethylammonium surfactants $C_nH_{2n+1}(CH_3)_3NBr$ have been used as structure-directing agents for zeolites, it has been found that shorter alkyl chain length surfactants (n=6 and 8) produced silicalite-1 at synthesis temperatures in the range of 150-200 ˚C. For the surfactants with longer chains (n=10-12), the silicalite-1-like zeolite crystals formed only at a higher temperature of 200 ˚C.[19] Notably, the surfactants with the longer chain lengths (n=14 and 16) failed to function as effective SDAs for zeolites (generating amorphous MCM-41-type silica).[19-24] On the other hand, Q. Li and co-workers found that silicalite-1, ZSM-5, mordenite, and ZSM-35 can be formed only at high temperatures above 170 ˚C with decreasing Si/Al ratios and proposed that the short chain alkylammonium species formed by decomposition of long chain surfactants led to the formation of these microporous zeolitic materials.[25-26] Therefore, the structure-directing formation of zeolites by quaternaries with longer alkyl chains, such as C14 and C16, under most conditions, is generally energetically unfavorable.[27-28] The use of longer chain quaternary surfactants to direct the formation of zeolites without decomposition may require particular organic-organic, organic-inorganic, and inorganic-inorganic interactions, which would provide an effective strategy to design rational routes to prepare molecular sieve materials.

In this study, we investigated the role of a long chain quaternary ammonium molecule, cetyltrimethylammonium bromide (CTAB), in the formation of zeolite ZSM-5. The particular synthesis composition was adjusted by varying the CTAB concentration, the SiO_2/Al_2O_3 molar ratio and so on. The macroscopic and the microscopic structures of the products were confirmed by X-ray diffraction (XRD) and scanning electron microscopy (SEM), and the existence (also the status and the amount) of CTAB in the pores was detected by IR spectroscopy, solid state ^{13}C NMR and elemental analysis.

Experimental

Chemicals

The silica source, tetraethyl orthosilicate (TEOS, 98%), was purchased from Sigma-Aldrich Company, Ltd. (USA). The quaternary ammonium surfactant CTAB, sodium aluminate and sodium hydroxide were obtained from Tokyo Chemical Industry (TCI), Ltd. (Japan). All materials were used as purchased without further purification.

Synthesis of zeolite materials Characterizations

In a typical synthesis of zeolite materials, the template or surfactant CTAB, sodium hydroxide, sodium aluminate and distilled water were mixed together while stirring. Then,

tetraethyl orthosilicate was added to give an original molar composition of CTAB: 20 SiO_2: 2.5 Na_2O: 0.2 Al_2O_3: 800 H_2O. The mixture was stirred for another 2 hours. Crystallization was carried out in Teflon-lined stainless steel autoclaves at 150 ˚C while tumbling at 40 r.p.m. After a crystallization period of 96 hours, the final products were filtered, washed with distilled water and dried at 100 ˚C overnight, and subsequently calcined in air at 550 ˚C.

Characterizations

Powder X-ray diffraction (XRD) patterns were recorded on a Rigaku X-ray diffractometer D/max-ⅢA equipped with Cu Kα radiation (40 kV, 30 mA). SEM was performed on a JEOL JSM-7401F electron microscope operated at 1 kV. The FT-IR spectra were recorded using a Perkin-Elmer Spectrum 100 FT-IR spectrometer. The ^{13}C CP/MAS NMR spectra were collected on an Oxford AS400 NMR spectrometer at 100 MHz with a sample spinning frequency of 3 kHz. Thermogravimetric analysis (TG) was performed with a Perkin-Elmer TGA7. The ratios of Si/Al in the samples were determined from the results of inductively coupled plasma analysis (ICP, Perkin-Elmer 3300DV) and elemental analysis of C, H, and N (Elementar Vario-ELIII IRMS analyzer). The nitrogen adsorption-desorption isotherms were measured at 77 K using an ASAP 2010 M+C analyser. The surface area was calculated by the Brunauer-Emmett-Teller (BET) method.

Results and discussion

At first, with CTAB as the SDA, we found that ZSM-5 can be synthesized at a wide temperature range of 100-200 ˚C and with particular synthesis compositions. The key factors of the ZSM-5 formation have been determined to be the CTAB/SiO_2, Na_2O/CTAB, and SiO_2/Al_2O_3 molar ratios, the compositions of which have been changed, while keeping the other factors constant to achieve the full synthesis conditions.

Figure 1 shows the XRD patterns and the SEM images of the products synthesized at different temperatures. At the lowest synthesis temperature (100 ˚C), a mixture of ZSM-5 and amorphous silica was obtained, according the low intensity of the XRD patterns and the crystalline- and amorphous-like morphologies in the SEM images. At 150 ˚C, the high-quality ZSM-5 was produced with no evidence of the formation of other zeolites or amorphous silica, as seen from its XRD pattern and SEM image. When the synthesis temperature was increased further (200 ˚C), the formation of a zeolitic mixture of ZSM-5 and a dense phase (alpha quartz) without any amorphous silica was evident. The formation of a zeolite with poor crystallinity and an amorphous mesophase at lower temperatures indicated that the solution energetics was only marginally favorable for the interactions of micelles and silicates (amorphous formation). At a higher temperature (200 ˚C), an undesirable, impure dense phase formed, which cannot contain the template.[29-30] Therefore, in the presence of longer alkyl chain quaternaries, the structure-directing formation of the ZSM-5 zeolite requires the proper SDAs content and energetic conditions. The temperature of 150 ˚C was considered to be the most appropriate for CTAB to direct the formation of ZSM-5 in the synthesis composition in this work.

To investigate the role of CTAB in the formation of ZSM-5, the synthesis was carried out with different molar ratios of CTAB/SiO_2 at 150 ˚C as shown in Figure 2. Although, MFI-like zeolitic materials were observed in the samples synthesized with

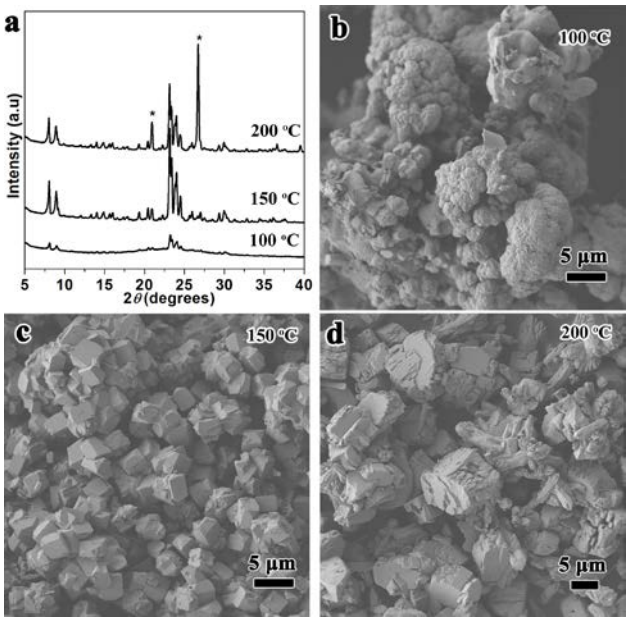

Fig. 1 The XRD patterns (**a**) and the SEM images of the zeolite products synthesized at different temperatures of 100 (**b**), 150 (**c**) and 200 ˚C (**d**). The synthesis molar composition was CTAB: SiO_2: Al_2O_3: Na_2O: H_2O = 1: 20: 0.2: 2.5: 800 with a crystallization period of 96 h. Diffraction peaks (labeled with *) at 200 ˚C belong to alpha quartz.

all CTAB/SiO_2 molar ratios tested here, even without CTAB, the pure high crystallinity ZSM-5 zeolites were synthesized with only limited CTAB/SiO_2 molar ratios of 0.025-0.05. In the presence of lower levels of CTAB, large amounts of lamellar silicate crystals that cannot contain organics formed, while many amorphous-like silica phases formed with higher CTAB contents, as seen from SEM images. Typically, the N/Si molar ratios were ~0.05 for the zeolitic products, whereas those forming the amorphous materials had ratios between 0.05 and 0.10.[31-33] In the CTAB synthesis system in this work, the N/Si molar ratios of the synthesis composition were in the range of 0.025-0.05 for the perfect ZSM-5 formation. The absence of CTAB would cause the formation of silicate, and an excess of CTAB would disrupt the high crystallinity ZSM-5.

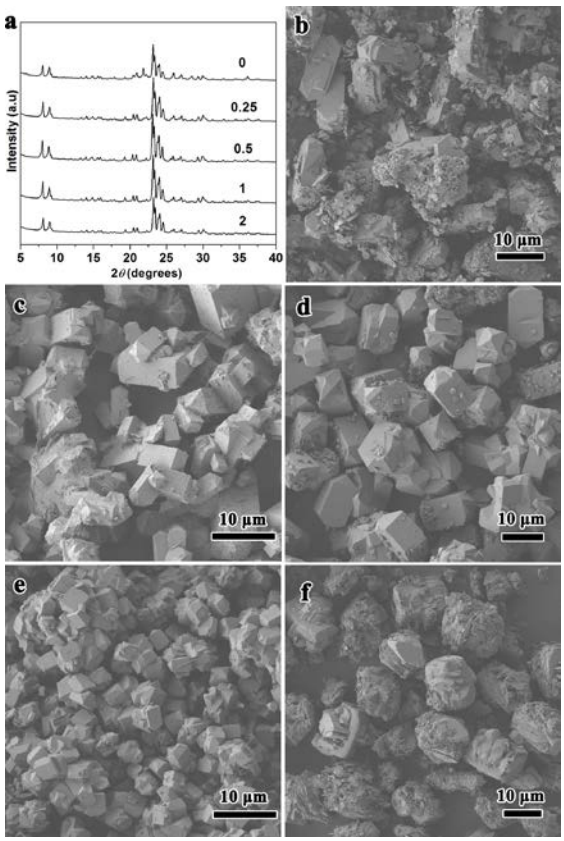

Fig. 2 The XRD (**a**) patterns and the SEM images of the zeolite materials synthesized with different amounts of CTAB added at 150 ˚C. The synthesis molar composition was CTAB: SiO_2: Al_2O_3: Na_2O: H_2O = x: 20: 0.2: 2.5: 800, where x= 0 (**b**), 0.25 (**c**), 0.5 (**d**), 1 (**e**), and 2 (**f**).

The SEM results for variations in the Si/Al molar ratios are shown in Figure 3. An appropriate Si/Al ratio was necessary for the formation of pure ZSM-5 crystals. As MFI-type zeolite is a kind of silica-rich microporous material, a low Si/Al ratio could result in the impure phase. From our results, the synthetic gel with ratios of Si/Al above 20 all can produce the pure ZSM-5 zeolite phase, although possessing different morphologies. Without adding of any aluminium source, silicalite-1 was also obtained under the similar synthesis composition (Figure 3f). It demonstrated that surfactant CTAB could be utilized to direct the formation of MFI type zeolite (ZSM-5 or silicalite-1) under proper original synthesis composition.

In order to study the existence of surfactant CTAB in the micropores, the ZSM-5 sample synthesized by the molar composition of SiO_2: Al_2O_3: Na_2O: H_2O = 1: 20: 0.2: 2.5: 800 under 150 ˚C after a crystallization period of 96 h (Figure 1) was employed for the detailed characterization as these described below. After calcination at 550 ˚C for 6 h, the N_2 adsorption-desorption isotherm of this sample exhibits a typical Langmuir-type curve (Figure 4) and the pore size distribution shows micropores centered around 0.54 nm, in good agreement with the typical micropore diameter of MFI-type zeolites, both indicating the presence of very uniform micropores. The Brunauer-Emmett-Teller (BET) surface area and pore volume are 385 m^2/g and 0.18 cm^3/g, respectively, similar to those of conventional ZSM-5. Combined with the XRD pattern and SEM image (Figures 1a and 1c), this ZSM-5 sample reveal a high crystallinity without any impurity. From the ICP analysis, the Si/Al ratio of this ZSM-5 sample is about 48, which approximates to the ratio in the original gel (50).

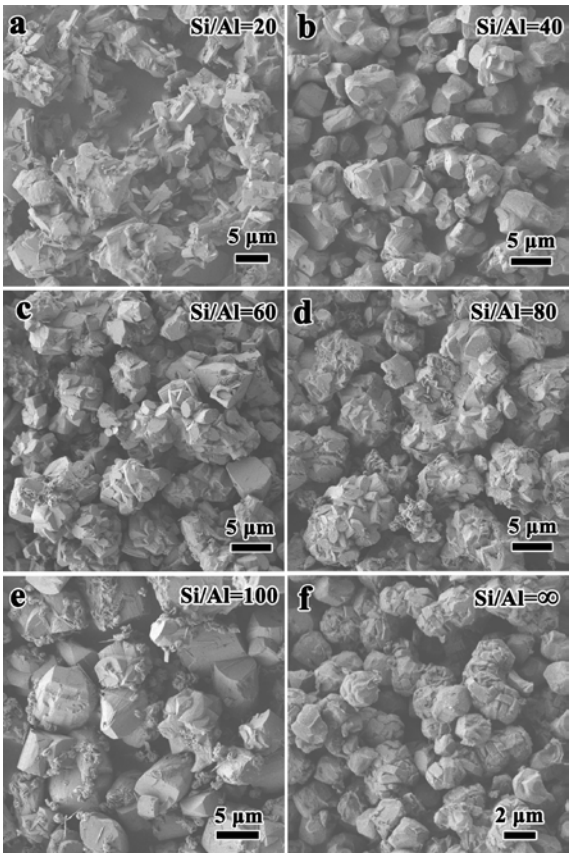

Fig. 3 SEM images of calcined materials synthesized by changing Al_2O_3 addition amount at 150 ˚C. The synthesis composition was CTAB: SiO_2: Al_2O_3: Na_2O: H_2O = 1: 20: x: 2.5: 800, where x=1/2 (**a**), 1/4 (**b**), 1/6 (**c**), 1/8 (**d**), 1/10 (**e**), 0 (**f**) (that is, Si/Al=20, 40, 60, 80, 100, ∞, respectively).

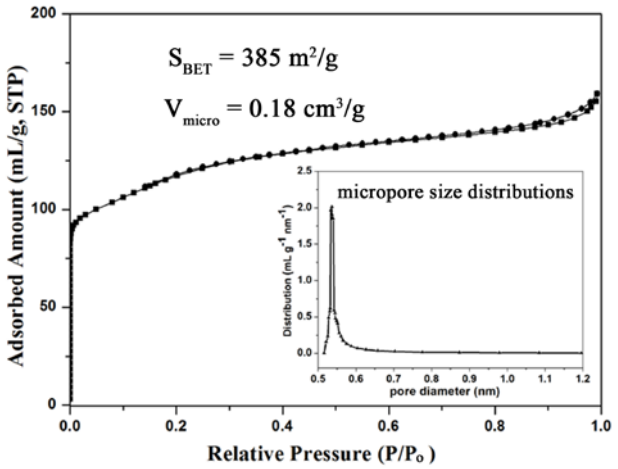

Fig. 4 N_2 adsorption-desorption isotherms and pore size distribution of the calcined ZSM-5 sample (Si/Al=48).

We carefully compared the IR spectra of CTAB in the as-prepared ZSM-5 sample to CTAB itself and CTAB in the MCM-41 material. The asymmetric and symmetric stretching bands (3016 and 2945 cm^{-1}) of the $N^+(CH_3)_3$ group were observed clearly in the IR spectra of powdered CTAB (Figure 5). When CTAB was introduced into ZSM-5 or MCM-41, the motion of the methyl groups was strongly restricted by the strong interactions between the silica framework and the quaternary ammonium.[34] As a result, the asymmetric stretching bands of the $N^+(CH_3)_3$ group disappeared, while the symmetric stretching bands (2959 cm^{-1}) were still present. The bands at 2918 and 2845 cm^{-1} belonged to the asymmetric and symmetric stretching bands of CH_2 groups. The bands (1243, 1061, 797, 597, 533 cm^{-1}) were attributed to the vibrations of T-O-T (T: Si or Al) in the framework of the zeolite or the mesoporous materials. In addition, no new bands were found, indicating that there were no new organic species different from CTAB in our synthesis system. The CTAB may pack perfectly in the final zeolite product to direct the formation of ZSM-5.

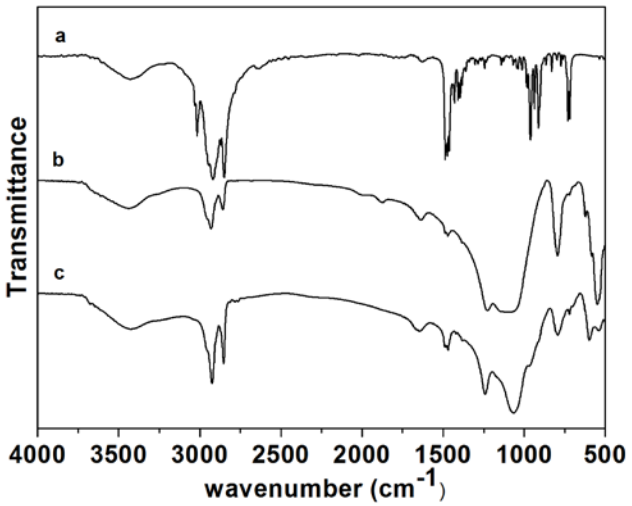

Fig. 5 IR spectra of CTAB as a crystalline solid (**a**), in the as-prepared ZSM-5 (**b**) and in the MCM-41 silica material (**c**).

The ^{13}C NMR spectra of CTAB in solution, as a crystalline solid, and in the as-prepared ZSM-5 sample are presented in Figure 6. The chemical shifts of the CTAB in solution can be easily distinguished and labeled according to the structural formula of CTAB. As the mobility and the environment of the carbon atoms in different situations is very influential, broader resonances with slight shifts were observed for CTAB in the crystalline powder compared to the solution, which is due to the higher packing density in the solid. With regard to the as-prepared ZSM-5 sample, the individual chemical shifts are similar to the solution case, although the resonances are broader than for the crystalline power. The similar broader chemical shifts suggested that the CTAB molecules were not packed densely but isolated from one other within the zeolite pores. Therefore, CTAB molecules were present and directed the speciation of the ZSM-5.

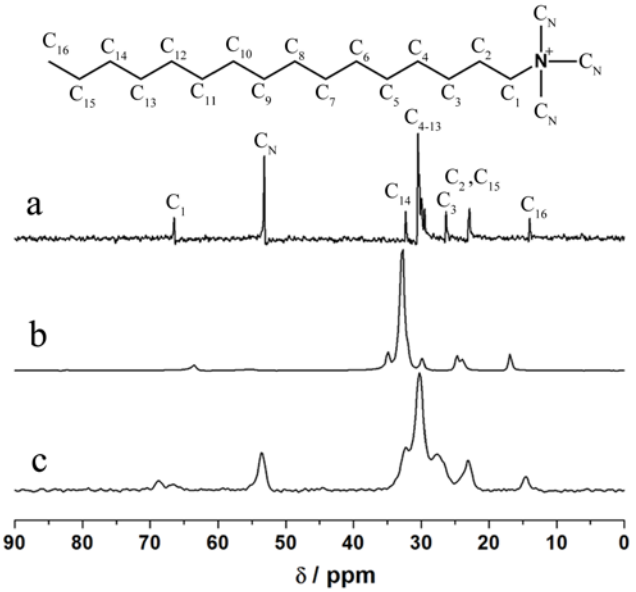

Fig. 6 ^{13}C NMR spectra of CTAB in D_2O solution (**a**), in the crystalline solid (**b**), and in as-prepared ZSM-5 synthesized at 150 °C (**c**).

The thermogravimetric curve (Figure 7) for the as-prepared ZSM-5 sample showed a distinct step for a loss in total weight (~20 %). The weight loss (~9.7 %) in the low temperature below 250 °C was related to the removal of intercrystalline water or residual template molecule which was not washed away as reported.[25, 35-36] The weight loss amounting to 10.2 % above 250 °C was due to the decomposition of the template CTAB. The elemental analysis of the as-prepared sample revealed that the C/N molar ratio (18.7) was approximately equal to the theoretical ratio in the template CTAB (C/N=19), which demonstrated that the template molecular was integrally located in the zeolite framework. As well known, in the conventional synthesis of ZSM-5 by tetrapropylammonium bromide (TPA), the maximum incorporation of TPA ions in per unit cell of MFI framework is about four. The unit cell contents of Na form is $Na_nSi_{96-n}Al_nO_{192}\cdot 16H_2O$ (n<27), while in our ZSM-5 material (Si/Al=48) is approximately $Na_2Si_{94}Al_2O_{192}\cdot 16H_2O$ (accurately n=1.96). That is, the idealized ratio of TPA to silicon from the composition of the as-prepared crystalline Si-ZSM-5 was about 0.042.[37-38] Compared to the ZSM-5 sample using CTAB as the SDA, an N/Si ratio of approximately 0.026 was obtained based on the precise elemental analysis. If ignoring the small quantity of Al, possible instrumental error and CTAB molecules adsorbed on the crystal surface, we can conclude that the incorporation of CTAB in per unit cell of our ZSM-5 sample was close to two. In this case, the final unit cell contents of our ZSM-5 material is $Na_2Si_{94}Al_2O_{192}\cdot 16H_2O\cdot 2CTAB$, where the mass weight of CTAB is 10.7 % which accords well with the TGA data. As the CTAB contains one ammonium head, only half of the total micropores were occupied by ammonium groups, while other species were present in the other half of the micropores.

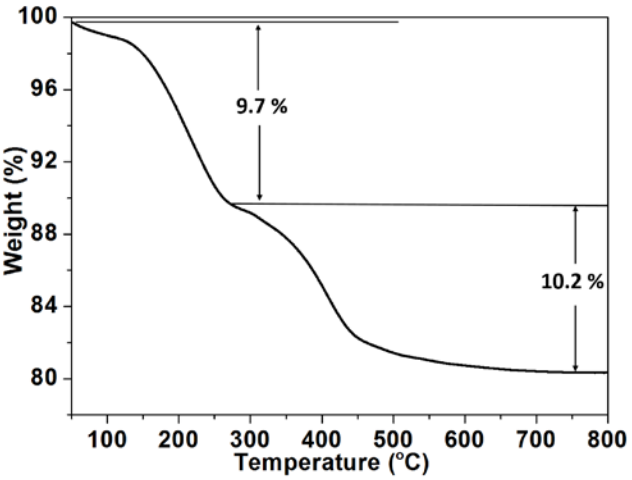

Fig. 7 TGA curves of as-prepared ZSM-5 synthesized with CTAB at 150 °C.

On the other hand, the cell parameters of MFI (orthorhombic system with *Pnma* space group) are a = 20.07 Å, b = 19.92 Å and c = 13.42 Å. Additionally, although the tail length of a single CTAB molecule is approximately 2.17 nm which seems to be longer than the distance of one unit cell along a or b axis,[39] the hydrocarbon chain is always flexible and easily transforms their configuration into some suitable manner. Because two sinusoidal 10-ring channels along a axis mismatch to be occupied by a CTAB molecule, the straight channels along the b-axis are the possible locations for the long chain surfactants as reported.[21-23] Based on the above results, we proposed a model for the location of CTAB molecules in the channels of the MFI zeolite. As shown in Figure 8, a single CTAB molecule participates in the formation of two micropores. The ammonium head acts as the SDA, and the hydrophobic tail plays the space-filling role. It is easy to visualize the structure-directing role of the trimethylammonium heads, whereas the location of hydrophobic tails is considered to readily occupy the adjacent pores along the b-axis of the MFI structure. We deduce that the tail of CTAB is space filling and directs the zeolite growth with trimethylammonium head simultaneously.

As the zeolite synthesis reaction is kinetically and/or thermodynamically controlled, the role of the surfactant CTAB during the crystallization growth of ZSM-5 can be characterized by the different interactions in the synthesis gel, for example, the inorganic-inorganic (II), the organic-inorganic (OI), and the organic-organic (OO) interactions.[40-42] At low temperatures, the interaction order is OI>OO>II, and the mesoporous phase can form based on the self-assembly of the surfactants. When the temperature is high enough, the organic-inorganic (OI) interactions dominate during the synthesis process with the interaction order of OI>OO and II>OO. Each surfactant molecule is encapsulated within the micropore framework with only secondary van der Waals organic-organic (OO) interactions. When a critical concentration of the inorganic-organic composite species is present, the aggregation of these species most likely leads to nucleation. The condensed silica precursor results in an enhanced rate of nucleation. Therefore, the microporous phases are finally produced. Under our synthesis conditions (150 °C and high pH), the CTAB molecules did not decompose, and they strongly interacted with the silica or the alumina. As a result, CTAB was able to direct the formation of micropores, which led to the growth of big zeolite crystals.

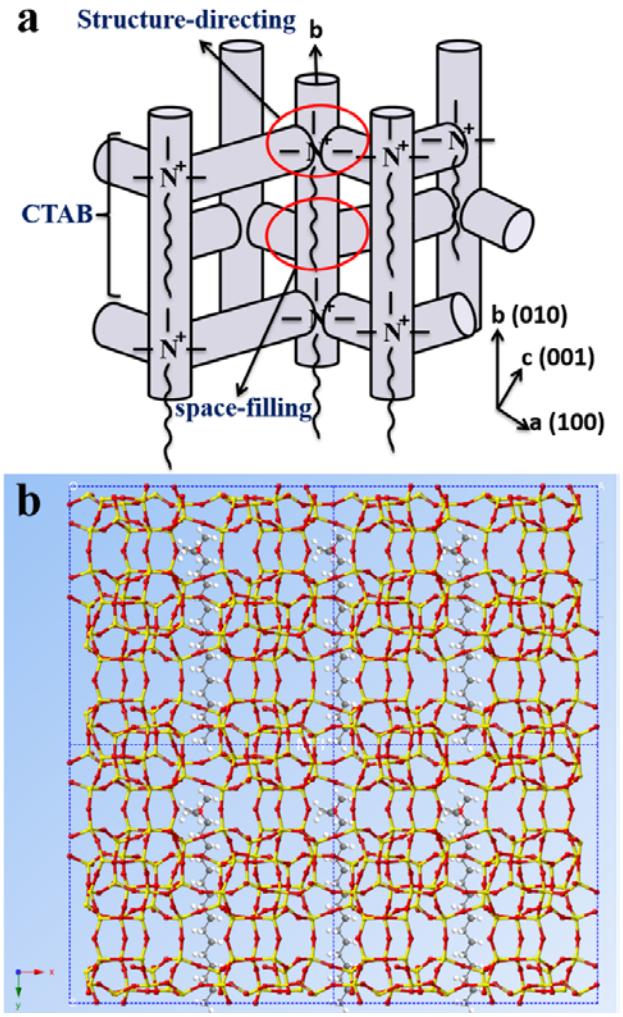

Fig. 8 Schematic illustration of the role of CTAB in the formation of MFI zeolite. **a**) The position of template CTAB illustrated in the three-dimensional MFI framework. **b**) The CTAB molecules (ball-and-stick model) located in the actual MFI unit cell along the (001) axis.

Conclusions

In summary, we successfully synthesized ZSM-5 by using the long chain trimethylammonium surfactant CTAB. The role of the CTAB surfactant was carefully studied. The characterization of the existence, status and content of CTAB in the micropores was performed by IR, ^{13}C NMR and elemental analysis. The results indicate that the CTAB surfactant act as a SDA without any decomposition, and the hydrophobic tail plays a space-filling role. To the best of our knowledge, this is the first time that this long chain quaternary ammonium molecule has been shown to function as an SDA in the production of zeolite materials. This finding may provide a new insight into the molecular factors governing the formation of inorganic-organic microporous materials, which would open up new possibilities for the fabrication of mesoporous zeolites.

Notes and references

School of Chemistry and Chemical Engineering, State Key Laboratory of Metal Matrix Composites, Shanghai Jiao Tong University, 800 Dongchuan Road, Minhang District, Shanghai, 200240, P. R. China
Fax: 86 5474 2852; Tel: 86 5474 5365; E-mail: chesa@sjtu.edu.cn
†These authors contributed to this work equally.

1 C. S. Cundy, P. A. Cox, *Chem. Rev.*, 2003, **103**, 663-702.
2 C. S. Cundy, P. A. Cox, *Micro. Meso. Mater.*, 2005, **82**, 1-78.
3 J. C. Jansen, in *Stud. Surf. Sci. Catal.*, Vol. Volume 137 (Eds.: E. M. F. P. A. J. H. van Bekkum, J. C. Jansen), Elsevier, 2001, pp. 175-227.
4 Y. Kubota, M. M. Helmkamp, S. I. Zones, M. E. Davis, *Micro. Mater.*, 1996, **6**, 213-229.
5 M. E. Davis, R. F. Lobo, *Chem. Mater.*, 1992, **4**, 756-768.
6 G. Sastre, S. Leiva, M. J. Sabater, I. Gimenez, F. Rey, S. Valencia, A. Corma, *J. Phys. Chem. B*, 2003, **107**, 5432-5440.
7 S. L. Lawton, W. J. Rohrbaugh, Science, 1990, **247**, 1319-1322.
8 Z. Wang, J. Yu, R. Xu, *Chem. Soc. Rev.*, 2012, **41**, 1729
9 J. Jiang, J. Yu, A. Corma, *Angew. Chem. Int. Ed.*, 2010, **49**, 3120-3145
10 A. P. Stevens, A. M. Gorman, C. M. Freeman, P. A. Cox, *J. Chem. Soc., Faraday Trans.*, 1996, **92**, 2065-2073.
11 B. Han, S.-H. Lee, C.-H. Shin, P. A. Cox, S. B. Hong, *Chem. Mater.*, 2005, **17**, 477-486.
12 R. J. Francis, D. O'Hare, *J. Chem. Soc., Dalton Trans.*, 1998, **0**, 3133-3148.
13 K. F. Domke, J. P. R. Day, G. Rago, T. A. Riemer, M. H. F. Kox, B. M. Weckhuysen, M. Bonn, *Angew. Chem. Int. Ed.*, 2012, **51**, 1343-1347.
14 I. D. Brown, D. Altermatt, *Acta Crystallographica Section B*, 1985, **41**, 244-247
15 X. Bu, P. Feng, G. D. Stucky, *Science*, 1997, **278**, 2080-2085
16 L. Wang, Y. Xu, Y. Wei, J. Duan, A. Chen, B. Wang, H. Ma, Z. Tian, L. Lin, *J. Am. Chem. Soc.*, 2006, **128**, 7432-7433
17 M. B. Park, Y. Lee, A. Zheng, F.-S. Xiao, C. P. Nicholas, G. J. Lewis, S. B. Hong, *J. Am. Chem. Soc.*, 2012, **135**, 2248-2255
18 J. Dedecek, V. Balgová, V. Pashkova, P. Klein, B. Wichterlová, *Chem. Mater.*, 2012, **24**, 3231-3239.
19 J. S. Beck, J. C. Vartuli, G. J. Kennedy, C. T. Kresge, W. J. Roth, S. E. Schramm, *Chem. Mater.*, 1994, **6**, 1816-1821.
20 C. T. Kresge, M. E. Leonowicz, W. J. Roth, J. C. Vartuli, J. S. Beck, *Nature*, 1992, **359**, 710-712
21 M. Choi, K. Na, J. Kim, Y. Sakamoto, O. Terasaki, R. Ryoo, *Nature*, 2009, **461**, 246-249
22 K. Na, C. Jo, J. Kim, K. Cho, J. Jung, Y. Seo, R. J. Messinger, B. F. Chmelka, R. Ryoo, *Science*, 2011, **333**, 328-332.
23 W. Park, D. Yu, K. Na, K. E. Jelfs, B. Slater, Y. Sakamoto, R. Ryoo, *Chem. Mater.*, 2011, **23**, 5131-5137.
24 F. Hasan, R. Singh, G. Li, D. Zhao, P. A. Webley, *J. Colloid and Interface Sci.*, 2012, **382**, 1-12.
25 L. Huang, X. Chen, Q. Li, *J. Mater. Chem.*, 2001, **11**, 610-615.
26 X. Chen, L. Huang, Q. Li, *J. Phys. Chem. B*, 1997, **101**, 8460-8467.
27 G. J. T. Tiddy, *Phys. Rep.*, 1980, **57**, 1-46.
28 P. A. Winsor, *Chem. Rev.*, 1968, **68**, 1-40.
29 X. Jiang, Y.-B. Jiang, C. J. Brinker, *Chem. Commun.*, 2011, **47**, 7524-7526.
30 J. F. Bertone, J. Cizeron, R. K. Wahi, J. K. Bosworth, V. L. Colvin, *Nano Lett.*, 2003, **3**, 655-659.
31 J. C. Vartuli, K. D. Schmitt, C. T. Kresge, W. J. Roth, M. E. Leonowicz, S. B. McCullen, S. D. Hellring, J. S. Beck, J. L. Schlenker, *Chem. Mater.*, 1994, **6**, 2317-2326.
32 J. C. Vartuli, C. T. Kresge, M. E. Leonowicz, A. S. Chu, S. B. McCullen, I. D. Johnson, E. W. Sheppard, *Chem. Mater.*, 1994, **6**, 2070-2077.
33 A. Burton, S. Elomari, R. C. Medrud, I. Y. Chan, C.-Y. Chen, L. M. Bull, E. S. Vittoratos, *J. Am. Chem. Soc.*, 2003, **125**, 1633-1642.
34 T. Kawai, J. Umemura, T. Takenaka, M. Kodama, Y. Ogawa, S. Seki, *Langmuir*, 1986, **2**, 739-743.
35 L. Parker, D. Bibby, J. Patterson, *Zeolites*, 1984, **4**, 168-174.
36 V. Shiralkar, A. Clearfield, *Zeolites*, 1989, **9**, 363-370.
37 S. L. Burkett, M. E. Davis, *Chem. Mater.*, 1995, **7**, 920-928.
38 K. Iwakai, T. Tago, H. Konno, Y. Nakasaka, T. Masuda, *Micro. Meso. Mater.*, 2011, **141**, 167-174.
39 G. Palazzo, F. Lopez, M. Giustini, *J. Phys. Chem. B*, 2003, **107**, 1924-1931.
40 H. Chon, S. K. Ihm, Y. S. Uh, Progress in zeolite and microporous materials, Vol. 105, Elsevier Science, 1996.
41 G. D. Stucky, Q. Huo, A. Firouzi, B. F. Chmelka, S. Schacht, I. G. Voigt- Schüth, *Stud. Surf. Sci. Catal.*, 1997, **105**, 3-28.
42 Q. Huo, D.I. Margolese, U. Ciesla, D.G. Demuth, P. Feng, T.E. Gier, P. Sieger, A. Firouzi, B.F. Chmelka, *Chem. Mater.*, 1994, **6**, 1176-1191.

SYNOPSIS TOC

Dongdong Xu†, Ji Feng†, Shunai Che*

Dalton Transactions. xxxx, xx, xxxx

An Insight into the Role of the Surfactant CTAB in the Formation of Microporous Molecular Sieves

ZSM-5 was synthesized by CTAB as structure-directing agent (SAD). The surfactant head groups can serve as SDA for zeolites and the long chains become isolated and occupy the micropores, which were in more rigid and did not undergo decomposition.